Colloid Polym Sci (2004) 282: 373–380
DOI 10.1007/s00396-003-0949-3

ORIGINAL CONTRIBUTION

Marc Laschet
Jan Philip Plog
Christian Clasen
Werner-Michael Kulicke

Examination of the flow behaviour of HEC and hmHEC solutions using structure–property relationships and rheo-optical methods

Received: 9 January 2003
Accepted: 19 May 2003
Published online: 6 August 2003

M. Laschet · J.P. Plog · C. Clasen
W.-M. Kulicke (✉)
Institute of Technical and Macromolecular Chemistry, Bundesstraße 45,
20146 Hamburg, Germany
E-mail: kulicke@chemie.uni-hamburg.de

Abstract The effect of solely intermolecular interactions due to hydrophobic alkyl substituents on the flow behaviour of hmHEC solutions was determined via comparison of the structure–property relationships of hmHECs and HECs based on the overlap parameter $c[\eta]$. For this purpose the η_0–$[\eta]$–c relationship for HEC was determined to be $\eta_0 = 8.91 \cdot 10^{-4} + 8.91 \cdot 10^{-4} \cdot c[\eta] + 1.07 \cdot 10^{-3} (c[\eta])^2 + 1.83 \cdot 10^{-7} (c[\eta])^{5.56}$. In addition the structure–property relationship for the longest relaxation time via the λ–$[\eta]$–c relationship $\lambda \cdot c^{1+1/a} = 2.65 \cdot 10^{-8} (c[\eta])^2 + 4.25 \cdot 10^{-8} (c[\eta])^3 + 5.44 \cdot 10^{-12} (c[\eta])^{5.27}$ has been determined. Although the hmHECs had a higher zero shear viscosity than HECs of comparable overlap parameters at a range of $1 < c[\eta] < 13$, the flow curves could be described via the same λ–$[\eta]$–c relationship in that range, indicating a timescale of the intermolecular interactions below the longest relaxation time.

The behaviour of the supramolecular structures in solution with an applied shear field was characterized by rheo-optical analysis of the shear thickening behaviour which occurs with addition of surfactant. Contrary to expectations, a slope >1 of the flow birefringence $\Delta n'$ as a function of shear rate could be observed in double logarithmic plotting. The degree of orientation of the flow birefringence ϕ primarily decreases with increasing shear rate, but increases later on at a characteristic shear rate. These two exceptional phenomena can be explained by a pronounced anisotropy of the polymer coils caused by the dilatant flow.

This assumption is backed up by the occurrence of a maximum in the dichroism curves which is caused by a finite stability of the aggregated structures in solution. On a molecular basis, these observations agree with the theoretically predicted (Witten and Cohen) transition from intra- to intermolecular polymer micelles. The detected aggregates correspond with the polymer chains that are aligned in one micelle.

Keywords Associative thickeners · Structure–property relationships · Shear thickening · Rheo-optics

Abbreviations

a	Exponent of the Mark–Houwink relationship
$c_{[\eta]}^*$	Critical concentration (determined by intrinsic viscosity)
c_{LS}^*	Critical concentration (determined by light scattering)
HASE	Hydrophobically modified alkali-swellable emulsions
HEUR	Hydrophobically modified ethoxylated urethanes
hmHEC	Hydrophobically modified hydroxyethylcellulose

HEC	Hydroxyethylcellulose
HPMC	Hydroxypropylmethylcellulose
M	Molecular mass
MS	Molar degree of substitution
n	Slope of the flow curve
SEC	Size exclusion chromatography
R_G	Radius of gyration
η	Viscosity
η_0	Zero-shear viscosity
η_{sp}	Specific viscosity
λ	Longest relaxation time
$\Delta n'$	Birefringence
$\Delta n'_i$	Intrinsic birefringence
$\Delta n'_f$	Form birefringence
$\Delta n''$	Dichroism
ϕ	Orientation of the birefringence
$\dot{\gamma}$	Shear rate

Introduction

In this work the flow behaviour of aqueous solutions of associative thickening, hydrophobically modified hydroxyethylcellulose (hmHEC) and hydroxyethylcellulose (HEC) (see Fig. 1) was characterized. While the structure of the HEC solutions can be described via the entanglement concept of Graessley [1], supramolecular structures in the hmHEC solutions, formed by the hydrophobic alkyl ether substituents, lead to a more complex flow behaviour.

HEC and hmHEC are deployed as thickening agents in water-based paints. Whereas HEC draws its thickening ability mainly from the entanglement interactions above c* [2], hmHEC belongs to the category of associative thickeners. The hydrophilic part enables the water solubility of the hmHEC, but the very small fraction of the hydrophobic compound provokes the associative thickening behaviour through associative interactions of the hydrophobic groups and the formation of a supramolecular structure in solution.

This supramolecular structure allows the production of paints which are superior to conventional products in terms of their sploshing behaviour. In addition there are patents for application of these associative thickeners in cosmetics [3, 4], paper conversion [5], drag reduction [6] and enhanced oil recovery [7].

The flow properties of hmHEC have been described by different authors [8, 9, 10], together with the zero-shear viscosity in comparison to unmodified HECs of the same chain length [11, 12]. However, in contrast to classic associative thickeners like HASE (hydrophobically modified alkali-swellable emulsions) and HEUR (hydrophobically modified ethoxylated urethanes), where the thickening effect depends primarily on the associative interactions of the side groups, for systems like HEC and hmHEC the dynamic of the polymer backbone adds to the viscosity and cannot therefore be neglected.

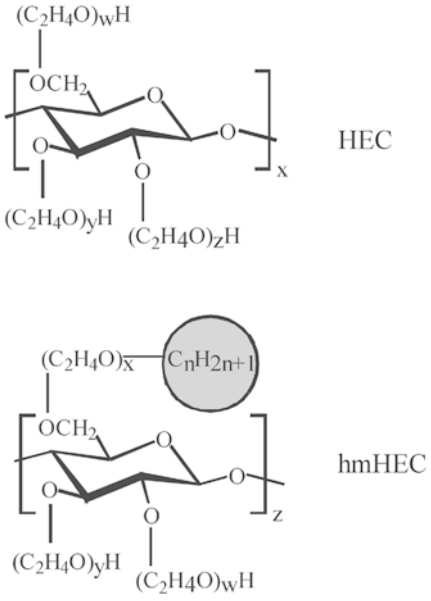

Fig. 1 Structures of hydroxyethylcellulose (HEC) and hydrophobically modified hydroxyethylcellulose (hmHEC)

So far there are no investigations reported that take into account the conformational change of the polymer backbone due to the intramolecular associative interactions of hydrophobic side groups. Even for backbones of the same type and length, these intramolecular interactions change the volume requirement for which the intrinsic viscosity [η] is a measure. One aim of this work is therefore to report the effect of a hydrophobic modification and intramolecular interaction on the flow parameters zero-shear viscosity and longest relaxation time depending on the overlap parameter c[η]. This is done on a series of HECs and hmHECs with different intrinsic viscosity and over a range of polymer concentrations.

In the presence of surfactants the supramolecular structure of associative thickeners in solution is altered, as reported for solutions containing hmHEC and sodium dodecyl sulfate (SDS) [12, 13, 14, 15, 16]. In the quiescent state the solution structure of mixtures of associative thickeners and surfactants could be characterized via fluorescence spectroscopy. With this method, as well as with DLS (dynamic light scattering) [11] and ILS (intensity light scattering) [17], the existence of mixed micelles of surfactants and associative thickeners could be verified [18]. These micellar structures lead to a complex alteration of the rheological material functions of the linear viscoelastic flow regime, depending on the surfactant solution concentration. In the non-linear viscoelastic shear, a dilatant (shear-thickening) behaviour of these solutions has been reported [15]. With

increasing concentration of surfactant the viscosity of a hydrophobically modified HEC increases, passes through a maximum and decreases again. At very high concentrations of surfactant the zero-shear viscosity can fall below the value of a surfactant-free solution [11, 12, 16]. With increasing concentration of polymer the concentration of surfactant where the maximum in viscosity shows up increases too.

Theoretical explanations of this shear-thickening behaviour are based on the micelle rearranging theories of Witten and Cohen [19], Ahn and Osaki [20] and Vrahopoulou and McHugh [21]. Until now there has been little experimentally proven information about the behaviour of micellar structures in a shear field at different shear rates. With rheo-optical techniques it is now possible to monitor the behaviour of a polymer chain as well as associated micellar structures on-line under shear. The flow birefringence and the orientation of the flow birefringence give detailed information about the dynamics and orientation of the individual polymer segments as well as associated structures. In particular, flow dichroism allows for predictions in terms of the size, stability and orientation of the micellar structures in the direction of the shear field.

The second aim of this paper is therefore to investigate the dynamic behaviour and the stability of the micellar structures of hmHEC under shear and to correlate this with the flow behaviour, the molecular parameters of this polymer and the theoretical predictions.

Experimental

Rheological measurements were accomplished on a controlled-rate rheometer Ares II (Rheometric Scientific, Piscataway, NJ, USA) and a controlled-stress rheometer UDS 200 (Physica Messtechnik, Stuttgart, Germany) with couette and cone and plate geometry in demineralized water. All measurements were carried out at 25 °C, only the rheo-optical measurements were carried out at 10 °C. For the determination of the structure–property relationships the polymers were dissolved in demineralized water under steady agitation for at least 4 days. For the rheo-optical investigations 1.5 cmc (critical micelle concentration) SDS was added (equals 0.36 wt%).

For rheo-optical measurements a self-constructed device with photoelastic modulation was used. For further information see [22, 23].

The MS (molar degree of substitution) and DS (degree of substitution) were determined via NMR spectroscopy and the intrinsic viscosities via viscosimetry. ^{13}C NMR spectroscopy was done at 100 °C in deuterated DMSO on an Advance 400 spectroscope (Bruker BioSpin GmbH, Rheinstetten, Germany). Before NMR was done, the samples were degraded with ultrasound to achieve a better resolution of the signals [24].

Determination of the molar mass, the molar mass distribution and the radius of gyration was done on a multi-angle light-scattering photometer with a coupled size-exclusion chromatograph (SEC). For fractionation, four SEC columns with decreasing exclusion size were used (TSK PW_{XL}: G3000, G4000, G5000, G6000, Toso-Haas, Stuttgart, Germany). These were coupled with a DAWN-F light-scattering photometer (Wyatt Technology, Santa Barbara, CA, USA) and a concentration detector Shodex RI SE-71 (Showa Denko, Tokyo, Japan). The solvent was demineralized, filtered water (0.1 μm pore diameter, Cellulose Filter, Sartorius) with 0.1 M $NaNO_3$ and 200 ppm NaN_3 as disinfecting agent.

The hmHECs were technical samples with alkyl substituents of 12–14 carbon atoms; both hmHEC and HEC samples were made available by Hercules (Wilmington, Delaware; USA).

A summary of the evaluated data is given in Table 1. Figure 2 shows the determined absolute molar mass distribution for the investigated HECs and hmHECs. It is worth noting that the samples HEC1 and hmHEC2 show the same molar mass distribution as well as the same MS, and are therefore ideally suited for an investigation of the effects of a hydrophobic modification on the flow behaviour. From the viscosimetric data the critical concentration $c_{[\eta]}^*$ was evaluated with Eq. 1 and c_{LS}^* was evaluated with Eq. 2 from the light scattering data [25].

$$c^* = \frac{2.5}{[\eta]} \tag{1}$$

$$c_{LS}^* = 1.31 \cdot 10^{-25} \frac{M_W}{R_G^3} \tag{2}$$

Table 1 Polymer analytical data from viscosimetry, SEC and MALS for the investigated HEC and hmHEC

	hmHEC1 HEC1	hmHEC2 HEC2	hmHEC3 HEC3	HEC4
M_w (10^6 g mol^{-1})	1.7	1.3	1.2	
M_w/M_n	1.13	1.5	1.44	
R_G (nm)	98	93	89	
$MS_{(HEC)}$	4.2	3.2	1.9	
$DS_{(hm)}$	0.063	0.039	0.012	
$[\eta]$ (cm^3 g^{-1})	1053	1213	1138	
c^*_{LS} (10^{-4} g ml^{-1})	2.3	2.3	2.1	
$c^*_{[\eta]}$ (10^{-3} g ml^{-1})	2.4	2.1	2.2	
M_w (10^6 g mol^{-1})	1.3	1.2	1.1	0.4
M_w/M_n	1.51	1.48	1.54	3.30
R_G (nm)	95	99	92	75
$MS_{(HEC)}$	3.1	3.1	3.0	3.0
$[\eta]$ (cm^3 g^{-1})	1231	1262	920	365
c^*_{LS} (10^{-4} g ml^{-1})	2.2	2.2	1.9	1.1
$c^*_{[\eta]}$ (10^{-3} g ml^{-1})	2.0	2.0	2.7	6.8

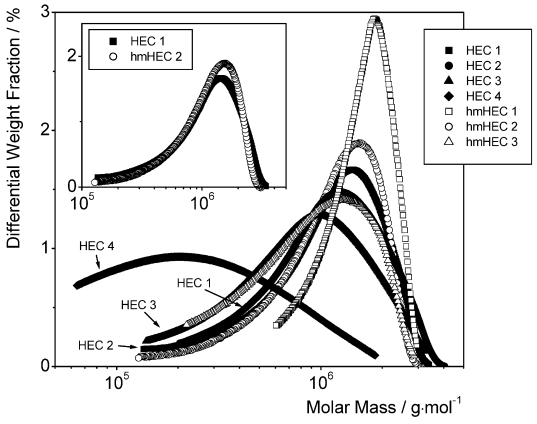

Fig. 2 Differential molar weight distribution of the investigated hydroxyethylcellulose (HEC) and hydrophobically modified hydroxyethylcellulose (hmHEC). The *insertion* shows that the molar weight distribution is nearly the same for HEC1 and hmHEC2

Results and discussion

The effect of hydrophobic modification of a cellulose derivative on its flow behaviour is not only determined by the intermolecular interactions between different coils that lead to supramolecular, three-dimensional networks. Even in dilute solutions, intramolecular interactions of the hydrophobic side groups of a single polymer coil lead to a change in the conformation of a hmHEC compared to an unmodified HEC.

For a comparison of the viscosity-enhancing three-dimensional network structure of hydrophobic modifications, the viscoelastic properties of hmHEC and HEC solutions are compared for similar intrinsic viscosities, rather than for similar molar masses or degrees of polymerization. The intrinsic viscosity is a measure of the volume requirement of a single polymer coil:

$$[\eta] = \lim_{\substack{c\to 0 \\ \dot{\gamma}\to 0}} \frac{\eta_{sp}}{c} \tag{3}$$

and has the unit of a reciprocal density of the polymer coil in the chosen solvent. The product of c and $[\eta]$, the so-called overlap parameter, is therefore a dimensionless number that refers to the volume requirement of the expanded polymer coils in solution. The correlation of viscoelastic properties with this overlap parameter allows for the determination of only the intermolecular interactions.

All other differences in the chemical structure, such as the DS and the MS (see Table 1), that affect the flow behaviour through changes in the conformational structure of the single coil are captured in the intrinsic viscosity $[\eta]$ [1, 26].

For the characterization of the viscous properties of a polymer fluid the zero-shear viscosity and the onset of the pseudoplastic area, determined by the longest relaxation time, are of crucial importance. Therefore the following structure–property relationships were chosen for a comparison of hmHEC and HEC. To quantify these effects over a range of solution structures, two sets of three hmHECs and four HECs with comparable molar mass ranges, but different polydispersities and MS (see Table 1), have been investigated over an overlap parameter range of 0.2–50.

η_0–$[\eta]$–c relationship

Bueche implemented a standardization for polymer melts that can be applied to polymer solutions of high concentration [27, 28]. The zero-shear viscosity is standardized over the product of concentration and molar mass ($c{\cdot}M_W$). Above a critical product $(c{\cdot}M_W)^*$ the slope of the zero-shear viscosity is 3.4, and below the critical product $(c{\cdot}M_W)^*$ the slope is 1. For semi-dilute solutions this plot delivers unsatisfying results since the molar mass does not incorporate any information on the expansion of the coil in solution.

According to an approach by Simha the specific viscosity η_{sp} of moderately concentrated solutions can be described as a function of the overlap parameter $c{\cdot}[\eta]$ [29]. A mathematical approach to this is a virial expansion where all exponents greater than two are combined in one term [30]:

$$\eta_{sp} = B_1 c\cdot[\eta] + B_2(c\cdot[\eta])^2 + B_n(c\cdot[\eta])^n \tag{4}$$

Comparison with the Huggins equation shows that the first two terms in Eq. 4 are identical to the Huggins equation and with $B_1 = 1$ and $B_2 = k_H$ one comes to:

$$\eta_{sp} = c\cdot[\eta] + k_H(c\cdot[\eta])^2 + B_n(c\cdot[\eta])^n \tag{5}$$

The third term describes the influence of polymer interactions in the moderately concentrated solution. The constants B_n and n can be determined by linear regression of the data for high values of the overlap parameter.

In Fig. 3 the specific viscosity η_{sp} of different aqueous HEC solutions is plotted versus the overlap parameter $c{\cdot}[\eta]$. A fit of this data set gives the η_{sp}–$[\eta]$–c relationship (Eq. 6):

$$\eta_{sp} = c\cdot[\eta] + 1.2(c\cdot[\eta])^2 + 0.205\cdot 10^{-3}(c\cdot[\eta])^{5.56} \tag{6}$$

Via the known Mark–Houwink relationship for HEC [31] and the relation $\eta_{sp} = \frac{\eta_0 - \eta_s}{\eta_s}$ Eq. 6 can be transferred into the η_0–M–c relationship

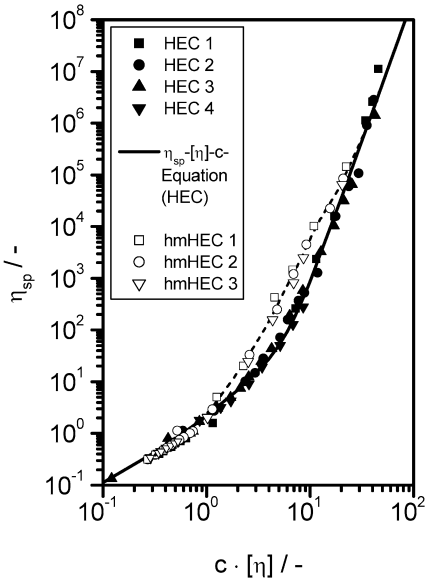

Fig. 3 Specific viscosity η_{sp} as a function of the overlap parameter c·[η] for HECs and hmHECs in aqueous solution. The *straight line* represents the fit according to the η_{sp}–[η]–c relationship (Eq. 6) for the HEC solutions

$$\eta_0 = 8.91 \cdot 10^{-4} + 3.6 \cdot 10^{-5} \cdot c \cdot M^{0.73} + 2.4 \cdot 10^{-6} \cdot c^2 \cdot M^{1.46} + 3.5 \cdot 10^{-12} \cdot c^{5.56} \cdot M^{4.06} \quad (7)$$

A fit of the hmHEC according to Eq. 6 is not possible, whereas at small overlap parameters the data seem to follow the same relationship as the unmodified HEC at intermediate overlap parameters.

λ–[η]–c relationship

Besides the area of zero-shear viscosity, which is described by the η_{sp}–[η]–c relationship, a shear rate-dependent area of the viscosity exists. The onset of this shear thinning region is characterized by a critical shear rate that equals the reciprocal of the longest relaxation time of the polymer in solution [32].

A first approach to explain the dependence of the relaxation time λ of a dilute polymer solution from the molar mass (M_W), concentration (c), temperature (T) and zero-shear viscosity (η_0) was done by Rouse and Ferry [33, 34].

$$\lambda_{R,p} = \frac{6}{\pi^2} \cdot \frac{(\eta_0 - \eta_s) M_W}{p^2 \cdot c \cdot R \cdot T};\ p = 1, 2, \ldots (N-1) \quad (8)$$

In the range of moderately concentrated solutions this model does not give satisfactory results. Observations show that in more concentrated solutions the longest relaxation time is shifted to longer times. This shift can be evaluated over a shift factor h [35].

$$\lambda_0 = h \cdot \lambda \quad (9)$$

In the area of the moderately concentrated solutions the shift factor h is a function of the molar mass M_W, concentration c and solvent quality a, that can be described empirically via Eq. 10 [36]:

$$h = \frac{\text{const.} \cdot [\eta]}{M_W \cdot c^{1/(a-1)}} \quad (10)$$

Substituting (η_0–η_s) with the η_{sp}–[η]–c relationship gives the λ–[η]–c relationship (Eq. 11). With this relationship the longest relaxation time can be determined from the intrinsic viscosity and the concentration.

$$\lambda_0 = K_\lambda \cdot c^{-(1+1/a)} \cdot \left((c \cdot [\eta])^2 + k_H \cdot (c \cdot [\eta])^3 + B_n \cdot (c \cdot [\eta])^{n+1} \right) \quad (11)$$

By plotting $\lambda_0 \cdot c^{(1+1/a)}$ versus the overlap parameter, the unknown constant K_λ can be determined through linear regression of the third term of Eq. 11 [37]. In Fig. 4 this is done for the HECs and hmHECs. From the plotted data, a λ–[η]–c relationship for HEC and hmHEC was determined:

$$\lambda \cdot c^{1+1/a} = 2.65 \cdot 10^{-8} \cdot (c \cdot [\eta])^2 + 4.25 \cdot 10^{-8} \cdot (c \cdot [\eta])^3 + 5.44 \cdot 10^{-12} \cdot (c \cdot [\eta])^{5.27};\ a = 0.61 \quad (12)$$

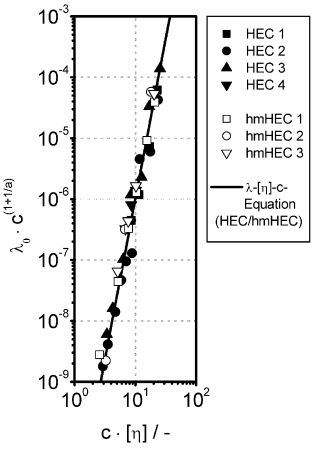

Fig. 4 Linear fit of the relaxation time-dependent term $\lambda_0 \cdot c^{(1+1/a)}$ as a function of the overlap parameter c·[η] for HECs and hmHECs in aqueous solution according to the λ_0–[η]–c relationship (Eq. 12)

Comparison of HEC with hmHEC

The η_{sp}–[η]–c relationship is ideally suited to compare the influence of a hydrophobic modification on the intrinsic viscosity since the influence of the molar mass

as well as the MS is taken into account by using the intrinsic viscosity. In Fig. 3 the specific viscosity of the HECs and hmHECs is plotted versus the overlap parameter. Compared to the determined η_0–[η]–c relationship for HEC, in the lower region of the curve, no deviation can be observed. For an overlap parameter >1 the specific viscosity of the hmHECs does clearly exceed that of the HECs. In this region, above the critical concentration c*, the hmHEC has a higher zero-shear viscosity than the HEC at the same concentration and coil dimensions, caused by the intermolecular interactions of the hydrophobic side chains. Due to this pronounced rise in η_0 above c* it is not possible to establish a simple structure–property relationship according to Eq. 7 that also covers the additional intermolecular interactions. At overlap parameters >13 the specific viscosity for hmHEC and HEC is again the same for comparable overlap parameters. In this regime the flow behaviour is dominated by the entanglements of the polymer backbone and the effect of the hydrophobic modifications on the viscosity are negligible.

Figure 4 shows that, via the plotted λ–[η]–c relationship, the longest relaxation times for both polymers are about the same for comparable intrinsic viscosities and overlap parameters.

Thus, intermolecular interactions via alkyl substituents enhance the zero-shear viscosity, but they do not have any influence on the longest relaxation time of the polymer coil. This indicates that the timescale of the formation of the supramolecular structure due to the hydrophobic interactions is below the longest relaxation time of the single polymer coil.

Rheo-optical analysis of the dilatant behaviour

The addition of a surfactant leads to the occurrence of a dilatant flow behaviour in hmHEC solutions. A direct comparison between the viscosity and birefringence of a hmHEC solution with a solution of unmodified HEC is possible for the samples HEC1 and hmHEC2 that show the same molar mass distribution and MS, as can be seen in Fig. 2 and Table 1. Figure 5 shows the flow curves for different concentrations of hmHEC. At small shear rates the flow curves show a constant zero-shear viscosity or a decreasing viscosity at the beginning of the shear thinning regime. At high shear rates a strong increase in viscosity is detected. The jump in viscosity in this so-called dilatant regime increases with decreasing concentration in the logarithmic plot. The onset of the dilatant regime is shifted to lower shear rates with increasing concentration (indicated by arrows in Fig. 5). In this first regime of dilatancy, no direct increase in viscosity is observed but there is an inflection point of the absolute value of the slope of the flow curve.

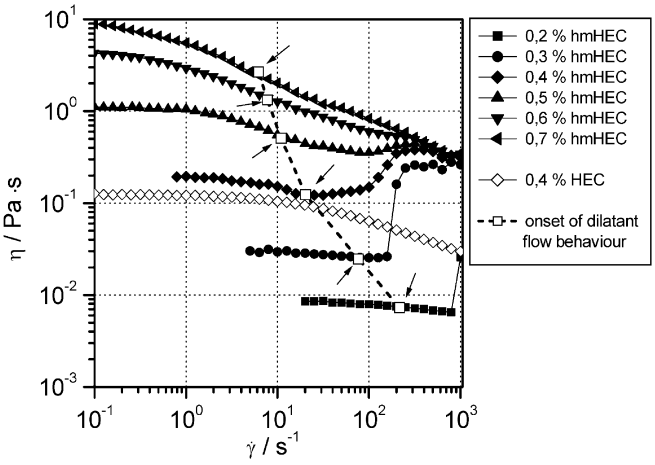

Fig. 5 Viscosity η as a function of the shear rate for different concentrations of hmHEC2 in aqueous solution with 0.36 wt% sodium dodecyl sulfate (SDS). The *open triangles* show the values for HEC1 at a concentration of 0.4 wt%. The *open squares* denote the onset of the dilatant flow behaviour

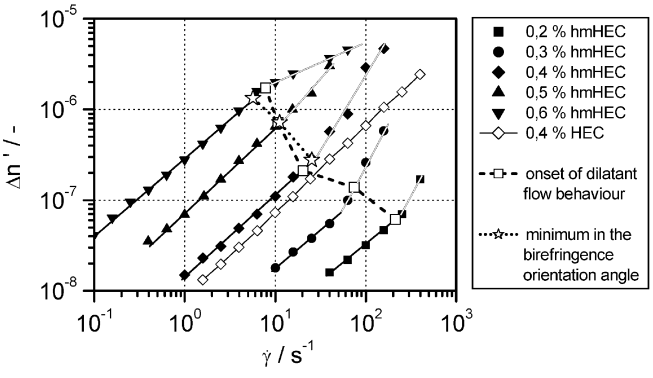

Fig. 6 Birefringence as a function of the shear rate for different concentrations of hmHEC2 in aqueous solution with 0.36 wt% sodium dodecyl sulfate (SDS). The *open triangles* show the values for HEC1 at a concentration of 0.4 wt%. The *open squares* denote the onset of the dilatant flow behaviour in Fig. 5. The *open stars* denote the minimum in the orientation angle values in Fig. 7

Comparison with the plotted data of the flow birefringence for these solutions (Fig. 6) shows that these inflection points (indicated by hollow squares) occur with an increase of the slope of the flow birefringence above a critical shear rate.

According to the stress–optical rule, the slope of the flow birefringence in the Newtonian regime should have an absolute value of 1 and an absolute value <1 in the non-Newtonian regime for ideal shear thinning solutions [38]. An increase in the slope to values greater than 1 indicates an increase in molecular interactions in terms of the shear-induced formation of supramolecular structures, as proposed by Tam et al. [39] via dynamic

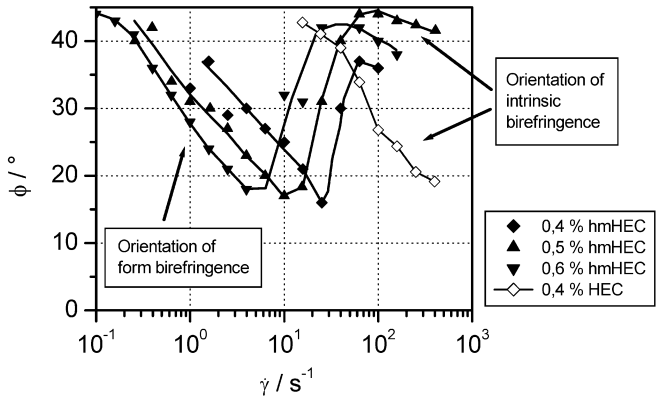

Fig. 7 Orientation of the birefringence as a function of the shear rate for different concentrations of hmHEC2 in aqueous solution with 0.36 wt% sodium dodecyl sulfate (SDS). The *open triangles* show the values for HEC1 at a concentration of 0.4 wt%

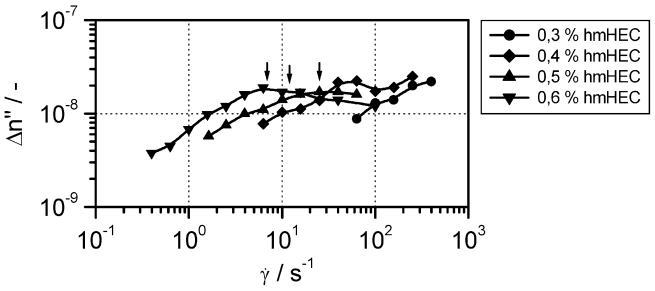

Fig. 8 Dichroism as a function of the shear rate for different concentrations of hmHEC2 in aqueous solution with 0.36 wt% sodium dodecyl sulfate (SDS)

oscillation experiments on steady flow. An increase in shear-induced intermolecular micelles leads to the dilatant behaviour and to the pronounced increase in the anisotropy and hence the flow birefringence.

A quantitative comparison between the viscosity and birefringence of the hmHEC solution with a solution of unmodified HEC that shows the same molar mass distribution and MS is done in Fig. 6 for solutions of 0.4 wt%. Without hydrophobic modifications a systematic decrease of the viscosity and birefringence occurs, as expected from the comparison of the structure–property relationship in Fig. 3. In addition, no dilatancy and no amplified anisotropy occur in the unmodified HEC above the critical shear rate.

Consideration of the degree of orientation of the birefringence allows a sophisticated view on the behaviour of the anisotropy in hmHEC solutions. In contrast to what was expected, the degree of orientation towards the direction of flow (0°) does not show a pronounced increase at the beginning of dilatancy, but decreases. As one can see in Fig. 7 the orientation angle undergoes a minimum before it increases again at higher shear rates. A comparable behaviour was found by Tassin [40] for associative thickening systems and by Clasen [41] for aggregated systems. Both authors assign this high degree of orientation at low shear rates to the strong anisotropy of aggregates in solution, that dominates the birefringence signal at low shear rates in terms of form birefringence $\Delta n'_f$. According to Fuller [42] the birefringence is made up of two fractions, the form birefringence caused by aggregates and an intrinsic birefringence $\Delta n'_i$ originating from the anisotropic orientation of the polymer segments:

$$\Delta n' = \Delta n'_f + \Delta n'_i \tag{13}$$

At high shear rates the intrinsic birefringence of the polymer segments dominates, because of the additional anisotropy of the intermolecular interactions, and leads to high values of the orientation angle (low orientation). This orientation angle decreases again (higher orientation) with increasing shear rate and increasing anisotropy. Comparison with the orientation of the unmodified HEC in Fig. 7 supports this interpretation of the orientation trend. The HEC shows a straight intrinsic trend for the birefringence without any aggregation. Orientation itself occurs, therefore, at considerably higher shear rates and is in good agreement with the intrinsic fraction of the orientation of the hmHEC. The shear rate that corresponds with the minimum value of the orientation of hmHEC taken from Fig. 7 is also plotted in Fig. 6 (open star symbols). As one can see these shear rates are in good agreement with the onset of the dilatancy. The behaviour of the aggregates can be considered apart from the intrinsic fraction via the form dichroism that is caused by a scattering on particles in the regime of visible light [42]. As shown in Fig. 8 the dichroism increases with an increasing shear rate, as expected for an anisotropic deformation and orientation of aggregates in the shear field. Above the shear rate of the onset of dilatancy, the value of the form dichroism remains constant or decreases slightly again. In this shear rate regime the aggregates reach their maximal deformation. The stresses are high enough to break the aggregates up and rearrange their structure.

The observation of these deforming and rearranging aggregated structures supports the theory of shear-induced transition from intra- to intermolecular micelles as suggested by Witten and Cohen [43]. In this case the micelles formed by the hydrophobic alkyl substituents cause the form dichroism. Above the critical shear rate of the onset of dilatant flow these intramolecular micelles build a dynamic equilibrium between breakup and re-formation as shown in Fig. 9. Due to the increase of flow rate the contact rate of alkyl substituents of different coils increases, and therefore the re-forming of intermolecular micelles increases as shown in Fig. 9. This build-up of a three-dimensional network of coil-connecting micelles leads to the increase in the viscosity and a pronounced stretching of the polymer segments

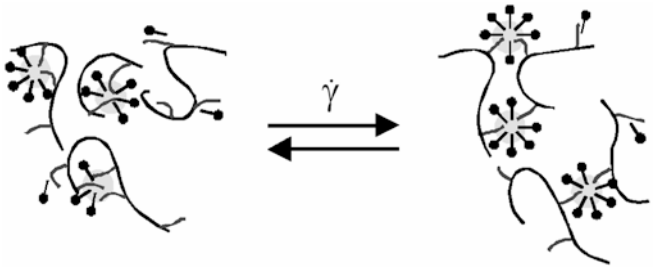

Fig. 9 Schematic figure of the shear rate-induced rearrangement from intra- to intermolecular micelles in aqueous hmHEC/SDS solutions

between these intermolecular micelles, and therefore to the increasing intrinsic birefringence with a slope >1 observed in Fig. 6.

Conclusion

It is shown in this paper that the hydrophobic modification of HEC leads to the build-up of supramolecular structures in aqueous solution. The existence of these supramolecular structures is reflected in the increase of the zero-shear viscosity for hmHEC in comparison with unmodified HEC. The relation of the zero-shear viscosity to the overlap parameter $c[\eta]$ allowed a qualitative determination of the viscosity enhancement due to only the intermolecular interactions of the hydrophobic side groups. The longest relaxation time of the solution is unaffected by the hydrophobic modification, indicating that the timescale of the supramolecular structure is below the longest relaxation time of the single polymer coil, as can be seen by comparing the λ–$[\eta]$–c relationships of hmHEC and HEC. Rheo-optical investigations of hmHEC solutions with surfactant show the occurrence of aggregates and give experimental support to the theoretically predicted (Witten and Cohen) transition from intra- to intermolecular polymer micelles in shear flow. Dichroism experiments show that these micelles rearrange above a critical shear rate to form the netpoints in a three-dimensional network. This supramolecular three-dimensional network causes the dilatant flow behaviour as well as a pronounced increase in the birefringence and orientation angle.

References

1. Graessley WW (1965) J Chem Phys 43:2696
2. Clasen C, Kulicke WM (2001) Prog Polym Sci 26:1839–1919
3. Chan AN, Clayton AB, Modi JJ (1998) US Patent 5,804,166
4. Bolich RE Jr, Norton MJ, Russel GD (1992) US Patent 5,104,646
5. Majewicz TG, Young TS (1991) US Patent 4,994,112
6. Bock J, Kowalik RM, Siano DB, Turner SR (1989) US Patent H577
7. Landoll LM (1985) US Patent 4,529,523
8. Sau A, Landoll LM, Odell JA, Keller A, Muller AJ (1989) Adv Chem Ser 223:343–364
9. Goodwin JW, Hughes RW, Lam CK, Miles JA, Warren BC (1989) Adv Chem Ser 223:365–378
10. Maestro A, Gonzalez C, Gutierrez JM (2002) J Rheol 46:127–143
11. Nyström B, Thuresson K, Lindman B (1995) Langmuir 11:1994–2002
12. Panmai S, Prudhomme RK, Pfeiffer DG (1999) Colloids Surf 147:3–15
13. Piculell L, Nilsson S, Sjösröm J, Thuresson K (1998) Abstr Pap Am Chem Soc 216:025-Cell Part 1
14. Sivadasan K, Somasundaran P (1990) Colloids Surf 49:229–239
15. Kaczmarski JP, Tarng MR, Ma Z, Glass E (1999) Colloids Surf 147:39–53
16. Picullel L, Guillement F, Thuresson K, Shubin V, Ericsson O (1996) Adv Colloid Interface Sci 63:1–21
17. Kjöniksen AL, Nilsson S, Thuresson K, Lindman B, Nyström B (2000) Macromolecules 33:877–886
18. Vorobyova O, Winnik MA (2001) Langmuir 17(5):1357–1366
19. Witten TA Jr, Cohen MH (1985) Macromolecules 18:1915–1918
20. Ahn KH, Osaki K (1994) J Non-Newtonian Fluid Mech 55:215
21. Vrahopoulou EP, McHugh AJ (1987) J Rheol 31(5): 371–384
22. Johnson SJ, Frattini L, Fuller GG (1985) J Colloid Interface Sci 104:440–455
23. Reinhardt UT, Meyer de Groot EL, Fuller GG, Kulicke WM (1995) Macromol Chem Phys 196:63–74
24. Baar A, Kulicke WM, Szablikowski K, Kiesewetter R (1994) Macromol Chem 195:1483
25. Kulicke, WM (1986) Fließverhalten von stoffen und stoffgemischen. Hüthig und Wepf, Heidelberg
26. Kulicke WM, Kull AH, Kull W, Thielking H, Engelhardt J, Pannek JB (1996) Polymer 37(3):2723–2731
27. Bueche F (1952) J Chem Phys 20:1959
28. Bueche F (1956) J Chem Phys 25:599
29. Simha R, Zakin L (1962) J Colloid Sci 17:270–287
30. Kulicke WM, Klare J (1980) Angew Makromol Chem 84:67
31. Bartsch S (1998) Charakterisierung kolloidaler systeme mittels größenausschlußchromatographie, querflußfraktionierung und lichtstreuung. Shaker, Aachen
32. Kulicke WM (1979) Macromol Chem 180:543
33. Rouse PE (1953) J Chem Phys 21:1272
34. Ferry JD (1978) Pure Appl Chem 50:299–308
35. Ferry JD, Landel RF, Williams ML (1955) J Appl Phys 26:359–362
36. Ferry JD, Landel RF, Williams ML (1955) J Appl Phys 26:359–362
37. Kulicke WM, Kniewske R, Müller RJ, Prescher M, Kehler H (1986) Ang Makromol Chem 142:29
38. Clasen C, Kulicke WM (2001) Rheol Acta 40:74–85
39. Tam KC, Jenkins RD, Winnik MA, Basset DR (1998) Macromolecules 31:4149–4159
40. Le Mein JF, Tassin JF, Corpart JM (1999) J Rheol 43:1423–1436
41. Clasen C, Kulicke WM (2002) J Rheol (in press)
42. Fuller GG (1995) Optical rheometry of complex fluids. Oxford University Press, New York
43. Witten TA Jr, Cohen MH (1985) Macromolecules 18:1915–1918